



HAL
open science

Discrimination of different amorphous carbon by low fluence laser irradiation

Hatem Diaf, Antonio Pereira, Patrice Melinon, Nicholas Blanchard, Florent Bourquard, Florence Garrelie, Christophe Donnet

► **To cite this version:**

Hatem Diaf, Antonio Pereira, Patrice Melinon, Nicholas Blanchard, Florent Bourquard, et al.. Discrimination of different amorphous carbon by low fluence laser irradiation. Carbon Trends, 2022, 9, pp.100195. 10.1016/j.cartre.2022.100195 . hal-03859200

HAL Id: hal-03859200

<https://hal.science/hal-03859200>

Submitted on 18 Nov 2022

HAL is a multi-disciplinary open access archive for the deposit and dissemination of scientific research documents, whether they are published or not. The documents may come from teaching and research institutions in France or abroad, or from public or private research centers.

L'archive ouverte pluridisciplinaire **HAL**, est destinée au dépôt et à la diffusion de documents scientifiques de niveau recherche, publiés ou non, émanant des établissements d'enseignement et de recherche français ou étrangers, des laboratoires publics ou privés.

Discrimination of different amorphous carbon by low fluence laser irradiation

Diaf Hatem^{a,*}, Pereira Antonio^a, Melinon Patrice^a, Blanchard Nicholas^a,
Bourquard Florent^b, Garrelie Florence^b, Donnet Christophe^b

^a*Université de Lyon, Université Claude Bernard, CNRS, Institut Lumière Matière UMR 5306, F-69622, Villeurbanne, France*

^b*Université de Lyon, Université Jean Monnet-Saint-Etienne, CNRS, Institut d'Optique Graduate School, Laboratoire Hubert Curien UMR 5516, F-42023, Saint-Etienne, France*

Abstract

Carbon thin film depositions were carried out with femtosecond laser ablation from two different sp^2 -bonded carbon targets, namely highly oriented pyrolytic graphite (HOPG) and glassy carbon (GC). Femtosecond laser deposition is generally known as a means of generating nanoparticles. To our knowledge, Raman spectroscopy is not able to directly discriminate the as-deposited amorphous films which may contain different sp^2 carbon nanoclusters while still showing similar Raman spectra. Moreover, these films are not easily distinguishable from each other by transmission electron microscopy observation due to their amorphous structure. In this work, we show that **controlled laser irradiation of thin films at low fluence is an interesting approach to reveal the existence of structural differences for amorphous films deposited from sp^2 carbon targets (HOPG and GC).**

1. Introduction

Thin films of amorphous carbon are a technologically interesting material due to **their highly adaptable** properties, which enable them to cover a wide range of industrial applications [1, 2, 3, 4]. **Their** physical properties are linked

*Corresponding author. Fax: +33 4 72 43 26 48.

Email address: hatem.diaf@univ-lyon1.fr (Diaf Hatem)

5 to the relative quantity of sp^3 , sp^2 and sp bonds and the network of atoms
connected to each other [5, 6]. For example, diamond-like carbon (DLC) is
well-known for its excellent mechanical and tribological properties due to the
high sp^3 content [7, 8]. DLC thin films can be obtained more easily with a
higher proportion of sp^3 by nanosecond laser deposition than by using a fem-
10 tosecond laser where the sp^3 content does not depend on the laser fluence [7].
Indeed, in femtosecond laser deposited films, the sp^3 content remains almost
unchanged at about 50% and 60% for a laser fluence ranging from 0.9 to 60
 J/cm^3 [9, 10, 11, 12, 13]. However, femtosecond laser ablation has proven to
be a suitable technique for the deposition of carbon nanoparticles, which is of
15 extreme interest for the realization of nano-devices [14, 15, 16]. For example,
Amoruso et al.[17] studied the optical emission of the plume from the ablation
in vacuum of a graphite target by femtosecond laser and evidenced the emis-
sion of the nanoclusters. Whatever the laser fluence used, thin films deposited
by femtosecond laser ablation are structurally amorphous [8, 18]. Unlike most
20 materials and due to a high degree of allotropy, it is therefore difficult or even
impossible to distinguish amorphous carbon films deposited from different 100%
 sp^2 -hybridised carbon targets, especially HOPG and GC. A complete knowledge
of the amorphous structure is extremely difficult to obtain using any character-
ization methods. Amorphous carbon density is often estimated using measured
25 sp^2/sp^3 hybridization ratios. However, it must be remembered that sp bonding
and nano-voids must be taken into account to obtain a complete description of
the microstructure of the amorphous carbon film. Moreover, they could possi-
bly contain the same relative amounts of the three hybridizations (sp^3 , sp^2 and
 sp) and have different structures. Also, unlike the sp^2 -bonded carbon (graphite,
30 carbon nanotubes, onions, fullerene, glassy carbon), amorphous structures are
not easily observable with transmission electron microscopy for comparison pur-
poses.

In this work, we show, based on Raman spectroscopy and XPS measure-
ments, that the laser-induced structural modification can be viewed as a new
35 way to discriminate different types of amorphous carbon.

2. Experimental

Amorphous carbon thin films were deposited on Si(100) substrates at room temperature under vacuum (5.10^{-6} mbar) or under helium pressure by femtosecond pulsed laser deposition (fs-PLD) using a pulsed Ti:sapphire laser (Coherent Legend Elite, wavelength $\lambda = 800$ nm, pulse duration = 50 fs and repetition rate $f = 1$ kHz). The laser was focused with an incident angle of 45° on one of the two used fully-sp² bonded carbon commercial targets (c.t): a glassy carbon target (Neyco, 99.9% purity, 1.54 g/cm³ mass density) or pyrolytic graphite target (Neyco, 99.9% purity, 2.27 g/cm³ mass density), labelled GC and HOPG respectively. Laser fluence was fixed to 13 J/cm² (high fluence) or 1 J/cm² (low fluence) for deposition under vacuum (5.10^{-6} mbar). For comparison purposes, a fluence of 1 J/cm² was also used for the films deposited by fs-PLD under 1 mbar of helium. **During deposition, the substrates** were placed parallel to the target surface at a distance of 3.6 cm. The substrates were previously ultrasonically cleaned in acetone and ethanol and then dried with dry nitrogen.

The deposited films were subsequently irradiated in air using the same femtosecond laser (fs-laser). The films deposited under vacuum (non-porous films) were irradiated with 500 pulses and a fluence ($F_{irradiation}$) of 0.07 J/cm², while the films deposited under 1 mbar of helium (porous films) were irradiated with 100 pulses and a fluence of 0.06 J/cm². These different values of fluence and number of laser pulses are due to the different mass density of the as-deposited films [19]. The second is less dense than the first and thus requires a lower irradiation energy to induce structural modification [19]. Indeed, the increasing background pressure leads to the formation of a porous structure (see Supplementary information Fig. S1).

Raman measurements were carried out with a 100× objective of 0.95 numerical aperture using an ARAMIS spectrometer (Horiba Jobin Yvon) and the unpolarized excitation energy of **a He-Ne laser at 633 nm**. Prior to data acquisition, the calibration of the spectrometer was made by taking into account the line of crystalline silicon at 520.5 cm⁻¹. The samples were analysed with a low

laser energy density to avoid laser-induced structural modifications during the measurements. The Raman signals from lattice vibrations of disordered carbon is sensitive to the degree of graphitization and to structural disorder which are determined by the ratio between the two bands I_D and I_G [20]. Multi-
70 wavelength unpolarised Raman and XPS measurements spectra were also acquired to measure the dispersion of the G band with the excitation wavelength and to estimate the sp^2 - sp^3 content on the surface of carbon films .

3. Results and discussion

Recently, we have successfully formed a glassy carbon thin film by controlled low fluence laser irradiation of a highly sp^3 -bonded DLC film previously
75 deposited on Si by ns-PLD under vacuum or 1 mbar of He [19](see Supplemental Material Fig.S4). Many studies use nanosecond lasers to irradiate amorphous carbon films in order to transform them into other forms of carbon (e.g. Q-carbon or reduced graphene oxide) [21, 22, 23]. The conversion to a given form
80 of carbon depends on the thermal conductivity of the substrate and the initial sp^3/sp^2 ratio [19, 21, 23]. In particular, sp^2 -rich amorphous carbon films deposited on Si (graphitizable carbon) can be graphitized to fully sp^2 ordered carbon such as graphene or graphite whereas sp^3 -rich amorphous carbon acts as a precursor for the synthesis of non-graphitizable carbon such as glassy carbon
85 [24, 23, 19].

We showed that sp^3 -rich carbon films deposited by ns-PLD from HOPG and GC c.t. (fully sp^2 -bonded carbon) with the same deposition conditions (under 1 mbar of He or under vacuum) are similar and can be transformed into the same structure of glassy carbon. They are morphologically different at the
90 macroscopic scale, but they have the same local structure at the microscopic scale [19]. In the present experiment, the femtosecond laser was used to study its ability to transform an as-deposited film under vacuum and 1 mbar of He into glassy carbon. The influence of the as-deposited nanoparticles on the film properties was also investigated.

95 *3.1. Carbon films deposited under vacuum by fs-PLD*

Carbon thin films deposited in vacuum by fs-PLD at the fluence of 13 J/cm^2 from the HOPG *c.t.* show an amorphous character characterized by a broad band centered around 1400 cm^{-1} , as shown on Fig.1(a). These films were subsequently exposed to femtosecond laser irradiation with 1 to 1000 shots and a fluence of 0.07 J/cm^2 . Figs.1(b)-(f) show the appearance of two separated and distinct peaks (D and G) under laser irradiation with 1 to 500 shots (Figs. 1 (b)-(e)) or with 1000 shots (Fig 1 (f)). The D and G bands are located at around 1330 cm^{-1} and 1600 cm^{-1} . Above 500 laser shots at 0.07 J/cm^2 , the shape of the spectrum in Fig. 1 (f) does not change, except for an increase of Si peak intensity, which indicates a decrease in the thickness of the carbon film and thus its ablation. At the same time, the I_D/I_G ratio increases with the number of laser shots to reach a value of 1.3-1.5 which remains constant above 500 shots. This indicates the formation of hexagonal rings of carbon atoms and of defects inside the nanocrystallites or at their edges [25, 20]. The optimal spectrum corresponds to a completely modified structure of the irradiated films and is characterized by the highest possible I_D/I_G ratio and the narrowest possible peaks, indicating a short/medium range crystal order. It is usually obtained just before the beginning of amorphization induced by laser irradiation or when the intensity of the Si peak starts to increase [19]. For these films, this therefore corresponds to an irradiation with 500 laser shots. In the following we focus only on the optimal spectra for comparison.

The same deposition conditions using two different targets (GC and HOPG *c.t.*) show similar results as highlighted in Figs.2 (b)-(c). Figure 2 suggests that the properties of the thin films do not depend on the nature of the sp^2 -hybridized carbon target, which is consistent with the literature [26]. Indeed, Orlianges et al. [26] have shown that thin films deposited by KrF laser ablation from GC and HOPG *c.t.* under the same experimental conditions have similar Raman spectra and sp^3 proportions.

Thin films were also deposited in vacuum by fs-PLD at a laser fluence of 1 J/cm^2 and subsequently irradiated with 500 shots at a fluence of 0.07 J/cm^2 .

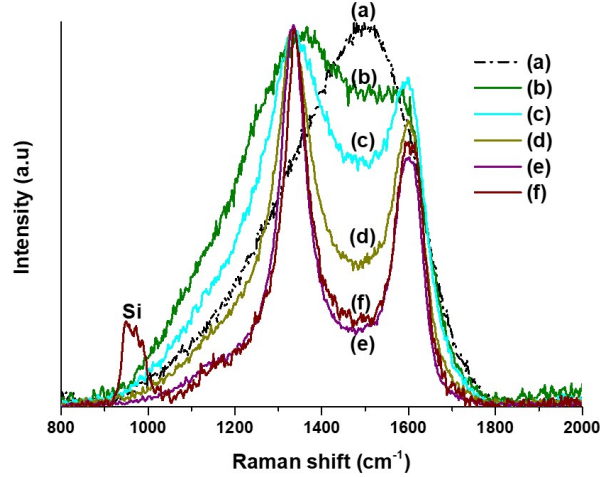


Fig. 1. Raman spectra of non-porous films deposited at 10^{-6} mbar with a laser fluence of 13 J/cm^2 from of the HOPG c.t. and irradiated at 0.07 J/cm^2 by fs-PLD with different number of laser pulses: (a) non-irradiated, (b) 1 shot, (c) 20 shots, (d) 50 shots, (e) 500 shots and (f) 1000 shots [19].

Fig.3 shows that the Raman signature of fs-deposited and fs-irradiated films does not depend on the energy density. It can therefore be assumed for the as-deposited films deposited in vacuum, that the laser fluence (13 J/cm^2 and 1 J/cm^2) has no influence on the structure obtained after irradiation (same Raman spectra and therefore same ordered structures are obtained). Nevertheless, the SEM images presented in Fig.4 show that with fs laser deposition, the presence of nanoparticles on the surface are more significant when using high fluence (13 J/cm^2 rather than 1 J/cm^2). The fs-laser therefore induces the ejection of particles from the target. This is due to the high shock of the fs-laser, which probably promotes mechanical spallation. All these results highlight that the properties of laser-irradiated films deposited under vacuum are weakly affected by the nature of sp^2 -hybridised carbon targets.

For a better comparison, the Raman spectra must be deconvoluted. For this, four components that contribute to Raman scattering are used: (i) the G peak at 1600 cm^{-1} typical of sp^2 carbon atoms, (ii) the D peak at 1330 cm^{-1}

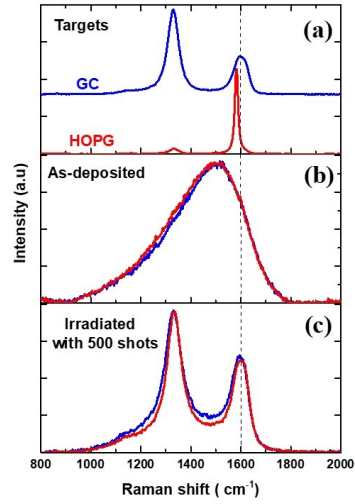


Fig. 2. Raman spectra of the GC (blue) and HOPG (red) c.t. (a) and of thin films deposited at 10^{-6} mbar at a laser fluence of 13 J/cm^2 by fs-PLD before (b) and after (c) laser irradiation with 500 shots at 0.07 J/cm^2 .

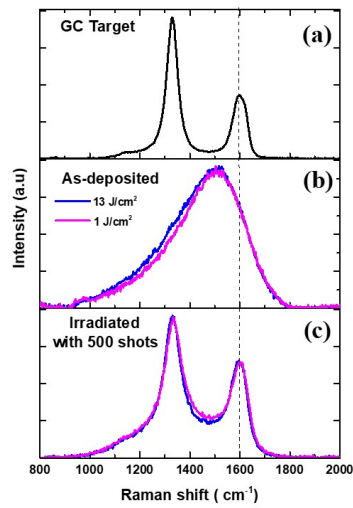


Fig. 3. Raman spectra of the GC c.t. (a) and of thin films deposited at 10^{-6} mbar by fs-PLD at two different laser fluences (1 and 13 J/cm^2) before (b) and after (c) laser irradiation at 0.07 J/cm^2 with 500 shots.

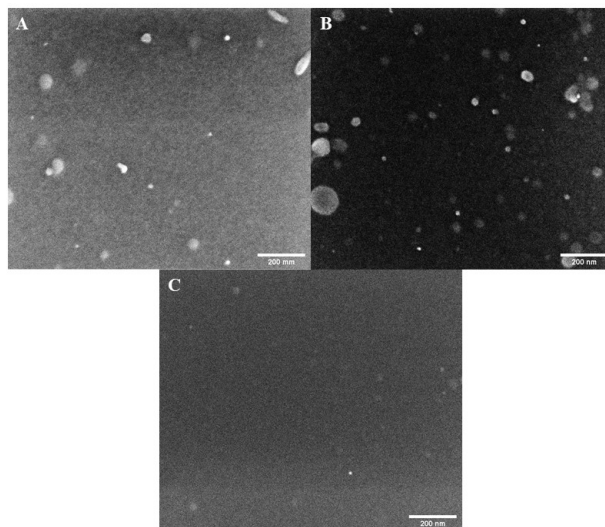


Fig. 4. SEM images of a carbon film deposited under vacuum by fs-PLD at a laser fluence of 13 J/cm^2 from GC (A) and HOPG (B) c.t. and at a fluence 1 J/cm^2 from GC c.t. (C).

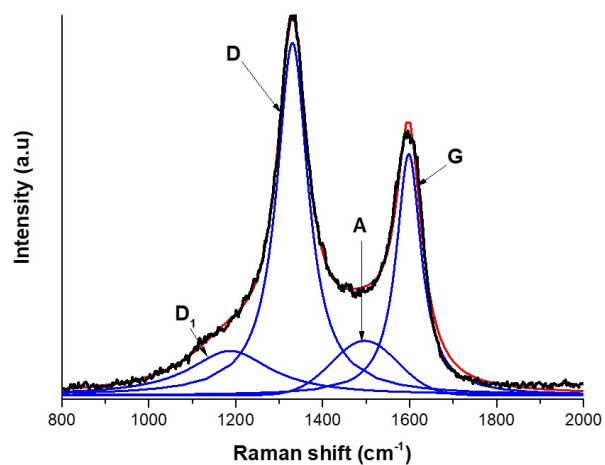


Fig. 5. Raman spectrum of a thin film deposited under vacuum by fs-PLD at 13 J/cm^2 from GC c.t. and irradiated by fs-laser at 0.07 J/cm^2 (black line). **Blues lines correspond to a Lorentzian for the G, D and D_1 bands, and a Gaussian for the A band. Red line represents the combination of four peaks.**

related to sp^2 atoms in hexagonal rings and to structural disorder, (iii) the D_1 peak at around 1200 cm^{-1} originating from the vibrations of nonhexagonal ring carbon defects (i.e., heptagons, pentagons, octagons) as described in [27, 28, 29, 30] and (iv) an A peak at 1500 cm^{-1} , which is necessary for a better fit and which is usually associated to amorphous graphitic phase bonded at sp^3 sites involving fragments, functional groups, and the presence of odd-membered rings and curvature [31, 32, 28, 33, 30]. This band is unfortunately not well understood. Here, for simplicity, the peak at 1620 cm^{-1} which is seen as a shoulder of the G peak is not included in the curve fitting. All spectra were fitted with three Lorentzian functions for the G, D and D_1 bands and a Gaussian function for the A band, as shown in Fig.5. **The choice of this fitting procedure is suitable for discriminating between the different amorphous carbons and it has been reported elsewhere [34].** The results of the Raman spectra fitting are summarized in the Table 1

Table 1 **shows** that regardless of the nature of sp^2 -hybridized carbon targets and the laser fluence, all the irradiated films deposited under vacuum are quite similar in terms of Raman parameters, with the exception of the FWHM of the D band. The three bands D, A and G are located at around 1330 cm^{-1} , 1490 cm^{-1} and 1599 cm^{-1} , **respectively**, with a I_D/I_G ratio between 1.4 and 1.5 and a A_A/A_G ratio between 0.3 and 0.4. The $FWHM_G$ value is about $70\text{-}75\text{ cm}^{-1}$ for all these films deposited from the two different sp^2 carbon targets, indicating a similar degree of ordering. In contrast, the $FWHM_D$ value is clearly higher for the films obtained from the GC **c.t.** ($88\text{-}92\text{ cm}^{-1}$) than for those obtained from **the HOPG c.t.** (74 cm^{-1}). The physical meaning of this discrepancy is unfortunately not well understood at present. Furthermore, compared to the GC and HOPG targets, the A_A/A_G ratio is higher for all irradiated films. This is probably due to the presence of a non-irradiated sub-layer or to the presence of a small amount of sp^2 -like clusters containing pentagonal sites such as fullerenes [30, 28]. The position of the G peak for the irradiated films is exactly the same as that of the GC **c.t.**, i.e. 1599 cm^{-1} (compared to 1583 cm^{-1} for the HOPG **c.t.**) and the I_D/I_G ratio is always higher than 1. According to these results,

Table 1: Results of the deconvoluted Raman spectra for the different films: fs-films deposited under vacuum and irradiated by fs-laser with 500 shots (N_{laser}) at 0.07 J/cm^2 ($F_{irradiation}$) from two different c.t. (GC and HOPG) at two different laser fluence ($F_{deposition}$) in J/cm^2 . Position (λ), full width at half maximum ($FWHM$) of D, A and G bands, respectively, area ratio (A_A/A_G) and intensity ratio (I_D/I_G) are given.

Sample	GC	HOPG	fs-film 1		fs-film 2
			GC	HOPG	GC
$F_{deposition}$			13		1
$F_{irradiation}$			0.07	0.07	0.07
N_{laser}			500	500	500
λ_T	1160		1188	1186	1197
$FWHM_T$	127		249	240	256
λ_D	1330	1333	1331	1334	1334
$FWHM_D$	53	42	88	74	92
λ_A			1497	1481	1482
$FWHM_A$			179	183	192
λ_G	1599	1583	1598	1599	1599
$FWHM_G$	59	15	70	70	75
A_A/A_G	0	0	0.4	0.3	0.4
I_D/I_G	2.1	0.1	1.5	1.4	1.4

amorphous carbon films can be seen as randomly distributed hexagon rings in a matrix of sp^3 -hybridized carbon and that can be transformed to glassy carbon structure by laser irradiation by converting the sp^3 sites to the sp^2 ones and forming curved graphene sheets interlinked between all dispersed hexagonal rings [19, 35]. fs-PLD under vacuum produces the same carbon films after laser irradiation, regardless of the sp^2 nature of the target.

3.2. Carbon films deposited in 1 mbar of helium by fs-PLD

In general, inert buffer gases are used to cool down and confine the ablation plasma where many physical processes take place (ionization, recombination processes, nucleation...etc.). Here, we have chosen to use helium to confine and cool down the ablation plasma because of its high thermal conductivity. Moreover, helium does not react chemically with carbon atoms and ensures a weak nucleation regime due to its low mass [36, 37].

Here, we introduced 1 mbar of helium into the deposition chamber to study its influence on the properties of carbon films deposited by fs-PLD from two different sp^2 hybridized carbon targets (GC and HOPG c.t.). For this purpose, we only used the experimental conditions where the films deposited in vacuum do not have particles on the surface, i.e. the films deposited at 1 J/cm².

The Raman spectra of the films deposited at 1 J/cm² in 1 mbar of helium by fs-PLD from the two different c.t. and irradiated with 100 laser pulses at a fluence of 0.06 J/cm² (highest I_D/I_G ratio and narrowest peaks corresponding to the best crystallisation) are shown in Fig.6. The results of the Raman spectra fitting are given in Table 2. As with the vacuum deposited films, Fig.6 shows that the Raman spectra of the as-deposited films under helium from the two different targets are apparently similar, but become surprisingly different after laser irradiation under the same conditions. These results emphasize that these films deposited from the two different sp^2 carbon targets are clearly different. In comparison with the films deposited in vacuum, the $FWHM_G$ increases by around 10 cm⁻¹ for the films deposited in helium, regardless of the nature of sp^2 hybridised carbon targets. This indicates a high stacking disorder or a high

amorphous character. But, the films deposited from the two different targets have the same degree of disorder. In contrast to the previous results, a significant difference between the two irradiated films in terms of the $FWHM_D$ and the A_A/A_G ratio is observed. It should be underlined that the $FWHM_D$ value increases by 30 and 100 cm^{-1} whereas the A_A/A_G ratio also increases by 0.3 and 0.6 for irradiated films deposited from the GC and HOPG c.t., respectively (see Tables 1 and 2). We can conclude that the $FWHM_D$ and A_A/A_G ratio are not related to the level of crystallization or disorder and indicate the presence of the sp^2 -like phases or clusters in the fs-PLD films deposited under helium. These phases associated to the A peak are chemically stable under laser irradiation and are more numerous in films deposited under helium than under vacuum. This is why films deposited under helium by fs-PLD cannot be transformed to a glassy-carbon like structure by laser irradiation. Furthermore, the A_A/A_G ratio is higher for films obtained from the HOPG c.t. (0.9) than for those obtained from the GC c.t. (0.7), evidencing the influence of the target when fs-PLD is performed under helium. Indeed, GC is a three dimensional network with strong C-C covalent bonds whereas HOPG is composed of graphenic sheets which are maintained together by weak Van der Waals forces. Consequently, the fs-laser shock removes graphene nanosheets from the HOPG c.t. more easily than from the GC one. Thus, the clusters embedded in the films from the HOPG c.t. seem to have a larger mean size than those from the GC c.t.. We assume that the $FWHM_D$ and the A_A/A_G ratio seem to depend on the mean size of the sp^2 fragments and their nature (HOPG and GC). The 1 mbar of helium pressure cools and confines the ablation plasma. Thus, it promotes the formation of sp^2 -like clusters from the different nucleus. These nucleus could probably be related to the nature of the target and prevent the thin films from changing to a glassy carbon structure under laser irradiation.

The dispersion of the G band with the excitation wavelength is sensitive to the degree of disorder [38]. The G band does not disperse in graphite and glassy carbon, whereas it does in disordered carbon materials. Casiraghi et al. [38] demonstrated a linear relationship between the G band dispersion and the

Table 2: Results of deconvoluted Raman spectra for the different films: **fs-He film 1** deposited at 1 mbar of helium and irradiated by fs-laser with 100 shots (N_{laser}) at 0.06 J/cm^2 ($F_{irradiation}$) from two different c.t. (GC and HOPG). Position (λ), full width at half maximum ($FWHM_D$) of D, A and G bands, respectively, area ratio (A_A/A_G) and intensity ratio (I_D/I_G) are given.

Sample	fs-He film 1	
	GC	HOPG
Helium pressure	1	
$F_{deposition}$	1	
$F_{irradiation}$	0.06	
N_{laser}	100	
λ_T	1208	1200
$FWHM_T$	280	302
λ_D	1334	1334
$FWHM_D$	122	178
λ_A	1500	1500
$FWHM_A$	186	192
λ_G	1599	1599
$FWHM_G$	80	87
A_A/A_G	0.7	0.9
I_D/I_G	1.3	1.3

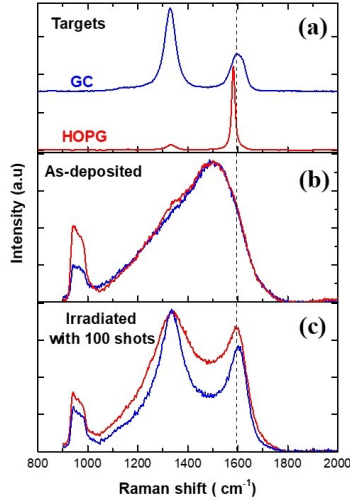


Fig. 6. Raman spectra of the GC (blue) and HOPG (red) c.t. (a) and of carbon thin films deposited by fs-PLD at the laser fluence of 1 J/cm^2 under 1 mbar of helium before (b) and after (c) fs-laser irradiation with 100 shots at the fluence of 0.06 J/cm^2 .

sp^3 amount. Our measurements (see Supplementary information Fig. S5) show that the non-irradiated films deposited under helium by fs-PLD from GC and HOPG c.t. have the same G band dispersion and thus the same sp^3 content [8]. According to this relationship, it can be estimated at about 50% (seen Supplementary information Fig. S6). These results are in agreement with XPS measurements, which show similar mixture of sp^2 and sp^3 sites with high fraction of sp^3 atoms, namely around 62% and 64% for the films deposited from the GC and HOPG c.t., respectively (see Supplementary information Fig. S7). On the other hand, it should be noted that this measurement is consistent with the same values of I_D/I_G obtained for these two cases. The absence of G band dispersion in the fully laser-modified films confirms that they are fully sp^2 -bonded. Surprisingly, the fs-laser deposited films in vacuum can be completely modified into glassy-carbon like structures by laser irradiation while the films deposited at 1 mbar of helium by the fs-laser cannot. These results show that the sp^2 -like phases are different in these two cases. The films that are likely to be transformed into glassy carbon like structure contain stable carbon clusters.

The formation of these clusters in the laser-induced plasma is consistent with the
250 formation of glassy carbon under laser irradiation, and in agreement with our
previous observations showing the existence of small fullerenes in the films [19].
The films which cannot be transformed into glassy carbon contain graphite-like
clusters originating from the ablation of the target. These results highlight the
presence of sp^2 -like clusters in the carbon film deposited by fs-PLD in helium
255 and the correlation with the nature of the target.

4. Conclusions

The simple approach combining pulsed laser deposition and subsequent laser
irradiation seems extremely useful to discriminate amorphous carbon which
could have the same hybridization content but with different sp^2 -like carbon
260 clusters (fullerenes, nanographites, nanocones, nanotubes). **It finally permits to
reveal the property difference between the films deposited under helium from
different sp^2 carbon targets by fs-PLD while their Raman spectra seem to be
visually similar.** These results finally showed that the $FWHM_D$ and the A
band are not related to the degree of disorder but mainly to the nature of the
265 sp^2 -like clusters. The as-deposited carbon film can be described as a sp^3 car-
bon matrix where the sp^2 -like clusters are randomly embedded. fs-PLD under
vacuum produces the same ionized plasma whatever the nature of sp^2 carbon
targets leading to the formation of the glassy-carbon like structure by laser
irradiation. However, a 1 mbar surrounding pressure during deposition **could**
270 **affect the interaction process between the fs-laser and the sp^2 carbon target
and thus significantly influence the formation of sp^2 carbon clusters within the
amorphous carbon.** These results open up the possibility to better control and
tune the physical properties of amorphous carbon depending on the nature of
the sp^2 -like clusters.

275 **References**

- [1] A. Bullen, K. O'Hara, D. Cahill, O. Monteiro, A. V. Keudell, Thermal conductivity of amorphous carbon thin films, *Journal of Applied Physics* 88 (11) (2000) 6317–6320. doi:10.1063/1.1314301.
- [2] W. Duley, Refractive indices for amorphous carbon, *The Astrophysical Journal* 287 (1984) 694–696. doi:10.1016/j.diamond.2005.08.069.
- 280 [3] S. Adhikari, S. Adhikary, A. Omer, M. R. H. Uchida, T. Soga, M. Umeno, Optical and structural properties of amorphous carbon thin films deposited by microwave surface-wave plasma cvd, *Diamond and related materials* 15 (2006) 188–192. doi:10.1016/j.diamond.2005.08.069.
- 285 [4] Y. Miyajima, A. Adikaari, S. Henley, J. Shannon, S. Silva, Electrical properties of pulsed uv laser irradiated amorphous carbon, *Applied Physics Letters* 92 (2008) 152104. doi:10.1016/j.diamond.2005.08.069.
- [5] J. Robertson, Mechanical properties and coordinations of amorphous carbons, *Physical review letters* 68 (1992) 220. doi:10.1103/PhysRevLett.68.220.
- 290 [6] M. Capano, N. McDevitt, R. Singh, F. Qian, Characterization of amorphous carbon thin films, *Journal of Vacuum Science & Technology A: Vacuum, Surfaces, and Films* 14 (1996) 431–435. doi:10.1116/1.580101.
- [7] F. Garrelie, A. Loir, C. Donnet, F. Rogemond, R. Le Harzic, M. Belin, E. Audouard, P. Laporte, Femtosecond pulsed laser deposition of diamond-like carbon thin films for tribological applications, *Surface and Coatings Technology* 163 (2003) 306–312. doi:10.1016/S0257-8972(02)00481-4.
- 295 [8] A. Sikora, F. Garrelie, C. Donnet, A. Loir, J. Fontaine, J. Sanchez-Lopez, T. Rojas, Structure of diamondlike carbon films deposited by femtosecond and nanosecond pulsed laser ablation, *Journal of Applied Physics* 108 (2010) 113516. doi:10.1063/1.3510483.
- 300

- [9] A. Hu, M. Rybachuk, Q.-B. Lu, W. W. Duley, Femtosecond pulsed laser deposition and optical properties of diamond-like amorphous carbon films embedded with sp-bonded carbon chains, *Diamond and related materials* 17 (7-10) (2008) 1643–1646. doi:10.1016/j.diamond.2008.03.024.
- [10] A. Hu, M. Rybachuk, I. Alkhesho, Q.-B. Lu, W. Duley, Nanostructure and sp 1/sp 2 clustering in tetrahedral amorphous carbon thin films grown by femtosecond laser deposition, *Journal of Laser Applications* 20 (1) (2008) 37–42. doi:10.2351/1.2832869.
- [11] S. Wang, Y. Guo, X. Wang, Y. Cheng, H. Wang, X. Liu, Infrared antireflection dlc films by femtosecond pulsed laser deposition, in: 4th International Symposium on Advanced Optical Manufacturing and Testing Technologies: Advanced Optical Manufacturing Technologies, Vol. 7282, 2009, p. 72820R. doi:10.1117/12.830809.
- [12] F. Qian, V. Craciun, R. Singh, S. Dutta, P. Pronko, High intensity femtosecond laser deposition of diamond-like carbon thin films, *Journal of Applied Physics* 86 (4) (1999) 2281–2290. doi:10.1063/1.371043.
- [13] S. Roy, P. Papakonstantinou, R. McCann, J. McLaughlin, A. Klini, N. Papadogiannis, Bonding configurations in amorphous carbon and nitrogenated carbon films synthesised by femtosecond laser deposition, *Applied Physics A* 79 (4) (2004) 1009–1014. doi:10.1007/s00339-004-2616-z.
- [14] S. Amoruso, G. Ausanio, R. Bruzzese, M. Vitiello, X. Wang, Femtosecond laser pulse irradiation of solid targets as a general route to nanoparticle formation in a vacuum, *Physical Review B* 71 (3) (2005) 033406. doi:10.1103/PhysRevB.71.033406.
- [15] G. M. Herrera, A. C. Padilla, S. P. Hernandez-Rivera, Surface enhanced raman scattering (sers) studies of gold and silver nanoparticles prepared by laser ablation, *Nanomaterials* 3 (1) (2013) 158–172. doi:10.3390/nano3010158.

- 330 [16] P. Spinelli, M. Hebbink, R. De Waele, L. Black, F. Lenzmann, A. Polman,
Optical impedance matching using coupled plasmonic nanoparticle arrays,
Nano letters 11 (4) (2013) 1760–1765. doi:10.1021/nl200321u.
- [17] S. Amoruso, G. Ausanio, M. Vitiello, X. Wang, Infrared femtosecond
laser ablation of graphite in high vacuum probed by optical emission
335 spectroscopy, Applied Physics A 81 (5) (2005) 981–986. doi:10.1007/
s00339-004-3059-2.
- [18] N. Jegenyés, Z. Toth, B. Hopp, J. Klebniczki, Z. Bor, C. Fotakis, Fem-
tosecond pulsed laser deposition of diamond-like carbon films: The effect
of double laser pulses, Applied surface science 252 (13) (2006) 4667–4671.
340 doi:10.1016/j.apsusc.2005.07.085.
- [19] H. Diaf, A. Pereira, P. Melinon, N. Blanchard, F. Bourquard, F. Garrelie,
C. Donnet, M. Vondráček, Revisiting thin film of glassy carbon, Physical
Review Materials 4 (2020) 066002. doi:10.1103/PhysRevMaterials.4.
066002.
- 345 [20] A. Ferrari, J. Robertson, Interpretation of raman spectra of disordered and
amorphous carbon, Physical Review B 61 (2000) 14095. doi:10.1103/
PhysRevB.61.14095.
- [21] A. Bhaumik, J. Narayan, Nano-to-micro diamond formation by nanosecond
pulsed laser annealing, Journal of Applied Physics 126 (12) (2019) 125307.
350 doi:10.1063/1.5118890.
- [22] R. Sachan, S. Gupta, J. Narayan, Nonequilibrium structural evolution of
q-carbon and interfaces, ACS Applied Materials & Interfaces 12 (1) (2019)
1330–1338. doi:10.1021/acsami.9b17428.
- [23] S. Gupta, J. Narayan, Reduced graphene oxide/amorphous carbon p–n
355 junctions: nanosecond laser patterning, ACS applied materials & interfaces
11 (27) (2019) 24318–24330. doi:10.1021/acsami.9b05374.

- [24] S. Gupta, R. Sachan, A. Bhaumik, P. Pant, J. Narayan, Undercooling driven growth of q-carbon, diamond, and graphite, *MRS Communications* 8 (2) (2018) 533–540. doi:10.1557/mrc.2018.76.
- 360 [25] L. Cançado, M. D. Silva, E. Ferreira, F. Hof, K. Kampioti, K. Huang, A. Pénicaud, C. C.A. Achete, R. Capaz, A. Jorio, Disentangling contributions of point and line defects in the raman spectra of graphene-related materials, *2D Materials* 4 (2017) 025039. doi:10.1088/2053-1583/aa5e7.
- [26] J. Orlianges, C. Champeaux, A. Catherinot, T. Merle, B. Angleraud, Pulsed laser deposition of tetrahedral amorphous carbon films from glassy carbon and graphite targets: a comparative study, *Thin Solid Films* 453 (2004) 285–290. doi:10.1103/PhysRevB.61.14095.
- 370 [27] M. Couzi, J. Bruneel, D. Talaga, L. Bokobza, A multi wavelength raman scattering study of defective graphitic carbon materials: The first order raman spectra revisited, *Carbon* 107 (2016) 388–394. doi:10.1016/j.carbon.2016.06.017.
- [28] J. Ribeiro-Soares, M. Oliveros, C. Garin, M. David, L. Martins, C. Almeida, E. Martins-Ferreira, K. Takai, T. Enoki, R. Magalhães-Paniago, et al., Structural analysis of polycrystalline graphene systems by raman spectroscopy, *Carbon* 95 (2015) 646–652. doi:10.1016/j.carbon.2015.08.020.
- 375 [29] V. Paillard, On the origin of the 1100 cm⁻¹ raman band in amorphous and nanocrystalline sp³ carbon, *EPL (Europhysics Letters)* 54 (2) (2001) 194. doi:10.1209/epl/i2001-00105-4/meta.
- 380 [30] T. Fujimori, K. Urita, Y. Aoki, H. Kanoh, T. Ohba, M. Yudasaka, S. Iijima, K. Kaneko, Fine nanostructure analysis of single-wall carbon nanohorns by surface-enhanced raman scattering, *The Journal of Physical Chemistry C* 112 (20) (2008) 7552–7556. doi:10.1021/jp801416b.

- [31] T. Jawhari, A. Roid, J. Casado, Raman spectroscopic characterization
385 of some commercially available carbon black materials, *Carbon* 33 (1995)
1561–1565. doi:10.1016/0008-6223(95)00117-V.
- [32] J. Schwan, S. Ulrich, V. Batori, H. Ehrhardt, S. Silva, Raman spectroscopy
on amorphous carbon films, *Journal of Applied Physics* 80 (1996) 440–447.
doi:10.1063/1.362745.
- 390 [33] A. Cuesta, P. Dhamelinourt, J. Laureyns, A. Martinez-Alonso, J. D.
Tascón, Raman microprobe studies on carbon materials, *Carbon* 32 (8)
(1994) 1523–1532. doi:10.1016/0008-6223(94)90148-1.
- [34] A. Sadezky, H. Muckenhuber, H. Grothe, R. Niessner, U. Pöschl, Raman
395 microspectroscopy of soot and related carbonaceous materials: Spectral
analysis and structural information, *Carbon* 43 (2005) 1731–1742. doi:
10.1016/j.carbon.2005.02.018.
- [35] P. Mélinon, Vitreous carbon, geometry and topology: A holistic approach,
Nanomaterials 11 (7) (2021) 1694. doi:10.3390/nano11071694.
- [36] K. Al-Shboul, S. Harilal, A. Hassanein, M. Polek, Dynamics of c_2 formation
400 in laser-produced carbon plasma in helium environment, *Journal of Applied
Physics* 109 (2011) 053302. doi:10.1063/1.3555679.
- [37] P. Mélinon, Principles of gas phase aggregation, *Gas-Phase Synthesis of
Nanoparticles* 23 38 (10.1002) (2017) 9783527698417.
- [38] C. Casiraghi, A. Ferrari, J. Robertson, Raman spectroscopy of hydro-
405 genated amorphous carbons, *Physical Review B* 72 (2005) 085401. doi:
10.1103/PhysRevB.72.085401.